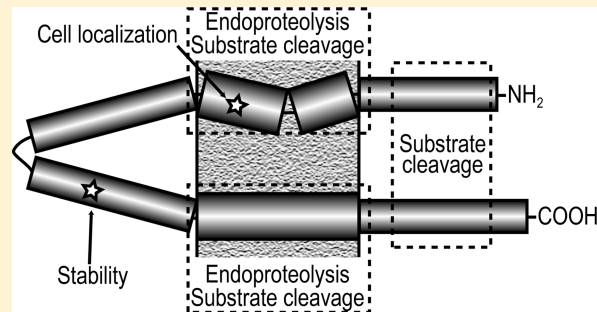


## Pen-2 Is Essential for $\gamma$ -Secretase Complex Stability and Trafficking but Partially Dispensable for Endoproteolysis

Oliver Holmes, Swetha Paturi, Dennis J. Selkoe, and Michael S. Wolfe\*

Center for Neurologic Diseases, Brigham and Women's Hospital and Harvard Medical School, Boston, Massachusetts 02115, United States

**ABSTRACT:** The 19-transmembrane  $\gamma$ -secretase complex generates the amyloid  $\beta$ -peptide of Alzheimer's disease by intramembrane proteolysis of the  $\beta$ -amyloid precursor protein. This complex is comprised of presenilin, Aph1, nicastrin, and Pen-2. The exact function and mechanism of the highly conserved Pen-2 subunit remain poorly understood. Using systematic mutagenesis, we confirm and extend our understanding of which key regions and specific residues play roles in various aspects of  $\gamma$ -secretase function, including maturation, localization, and activity, but not processivity. In general, mutations (1) within the first half of transmembrane domain (TMD) 1 of Pen-2 decreased PS1 endoproteolysis and  $\gamma$ -secretase proteolytic activity, (2) within the second half of TMD1 increased proteolytic activity, (3) within the cytosolic loop region decreased proteolytic activity, (4) within TMD2 decreased PS1 endoproteolysis, (5) within the first half of TMD2 decreased proteolytic activity, and (6) within C-terminal residues decreased proteolytic activity. Specific mutational effects included N33A in TMD1 causing an increase in  $\gamma$ -secretase complexes at the cell surface and a modest decrease in stability and the previously unreported I53A mutation in the loop region reducing stability 10-fold and proteolytic activity by half. In addition, we confirm that minor PS1 endoproteolysis can occur in the complete absence of Pen-2. Together, these data suggest that rather than solely being a catalyst for  $\gamma$ -secretase endoproteolysis, Pen-2 may also stabilize the complex prior to PS1 endoproteolysis, allowing time for full assembly and proper trafficking.



$\gamma$ -Secretase is a 19-transmembrane domain (TMD), intra-membrane aspartyl protease comprised of presenilin (PS1 or PS2 isoform) as the catalytic component,<sup>1</sup> along with nicastrin (Nct), anterior pharynx defective-1 (Aph1 $\alpha$ L, Aph1 $\alpha$ S, or Aph1 $\beta$  isoform), and presenilin enhancer-2 (Pen-2). All four components are necessary and sufficient for  $\gamma$ -activity.<sup>2–4</sup> The  $\gamma$ -secretase complex is responsible for the second and final step in regulated intramembrane proteolysis (RIP)<sup>5</sup> of a large and increasing number of substrates, the most studied of which are the  $\beta$ -amyloid precursor protein (APP) and Notch.<sup>6</sup> A further complexity of  $\gamma$ -secretase function is the fact that cleavage of the membrane-anchored C99 stub of APP (as a model  $\gamma$ -substrate) occurs at multiple sequential peptide bonds, starting with  $\epsilon$ -cleavage to release the APP intracellular domain (AICD) from the membrane and leave a 49- or 48-residue amyloid  $\beta$ -protein ( $A\beta$ ) peptide.<sup>7,8</sup> Sequential cleavages of  $A\beta_{48/49}$  every three or four residues moving N-terminally (i.e., every helical turn of the TMD) occur first at the so-called  $\zeta$ -site to produce  $A\beta_{45/46}$ , then at the  $\gamma$ -site to produce  $A\beta_{42/43}$ , and finally at the  $\gamma'$ -site to produce  $A\beta_{38/40}$  peptides.<sup>9</sup>  $A\beta_{42}$  is generally considered the most pathogenic (i.e., self-aggregating)  $A\beta$  species, with an elevated  $A\beta_{42}/A\beta_{40}$  ratio used as a marker of pathogenicity,<sup>10</sup> although recently,  $A\beta_{43}$  has also been shown to be pathogenically relevant *in vivo*.<sup>11</sup> The sequential C-terminal trimming of the initial  $\epsilon$ -cleavage products  $A\beta_{48}$  and  $A\beta_{49}$  by  $\gamma$ -secretase is termed processivity.<sup>12</sup>

Biochemical studies have previously shown that the Pen-2 subunit is the final component added to  $\gamma$ -secretase,<sup>4</sup> whereupon the PS holoprotein undergoes autoproteolysis<sup>1,13</sup> in a hydrophobic domain within the cytosolic loop between TMD 6 and 7 to form stable N-terminal and C-terminal fragments (NTF and CTF, respectively) that stay associated in the membrane as heterodimers.<sup>14</sup> The essential nature of Pen-2 was illustrated *in vivo* using Pen-2 knockout mice,<sup>15</sup> the embryonic lethal phenotype of which was very similar to that of a PS1/PS2 double knockout or a Notch1 knockout. Pen-2 is very highly conserved, being invariably 101 residues long with 70% identity and 87% similarity among all vertebrates and retaining 56% similarity between *Homo sapiens* and *Arabidopsis thaliana* (Figure 1a,b). Glycosylation studies were utilized to demonstrate that the topology of Pen-2 comprises luminal N- and C-termini, two TMDs, and a cytosolic loop region.<sup>16</sup> The first of these two TMDs was previously reported to be important for interaction with TMD 4 of PS1<sup>17,18</sup> and was more recently localized to a water-accessible pore.<sup>15</sup> The cytosolic loop region of Pen-2 is apparently accessible from the luminal side of membranes via a hydrophilic cavity and may interact with PS1-CTF.<sup>15</sup>

Received: April 24, 2014

Revised: June 17, 2014

Published: June 18, 2014

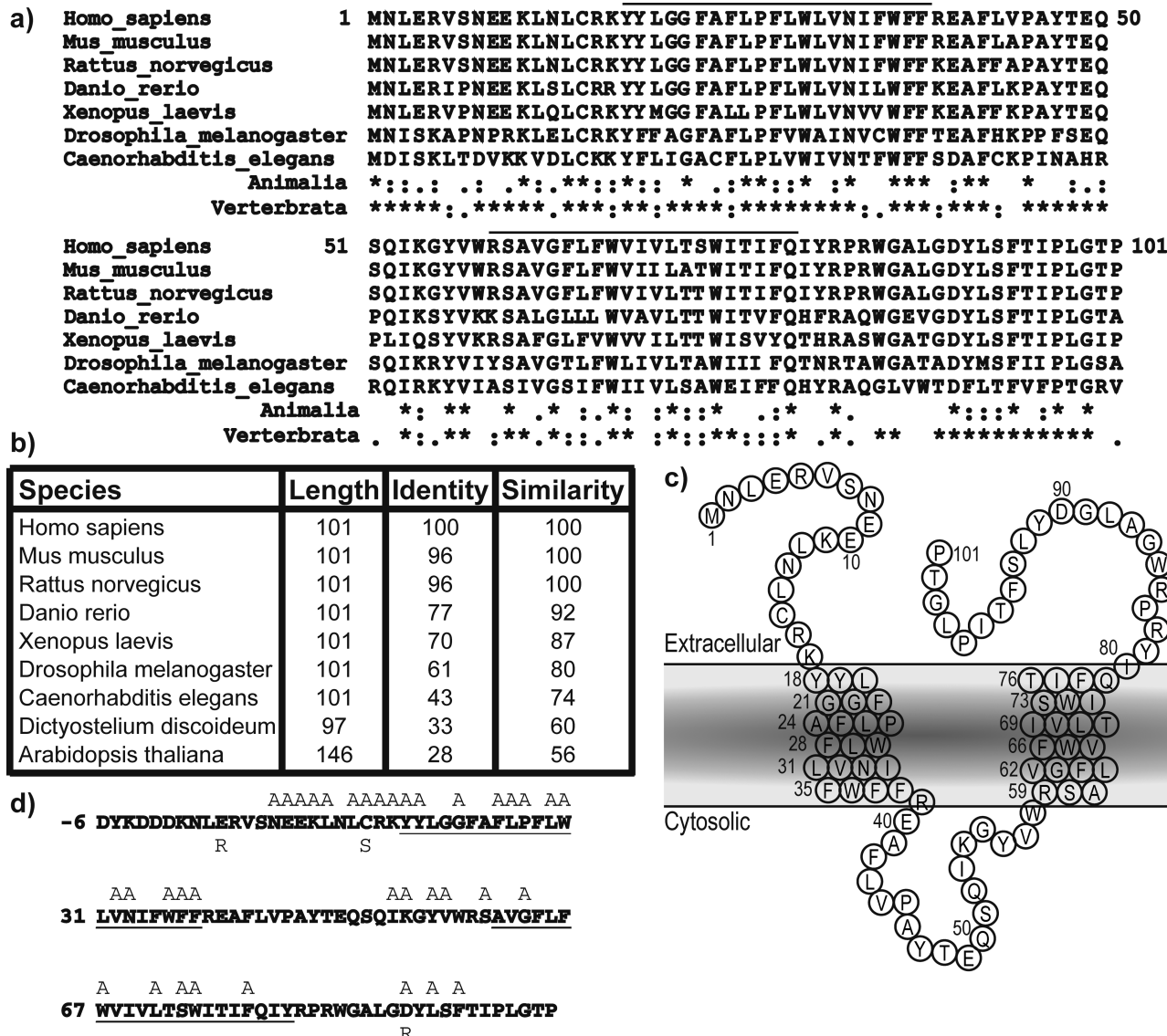


**Figure 1.** Sequence conservation of Pen-2. (a) Multiple-sequence alignment of forms of Pen-2 from various model organisms. The black bar denotes the predicted transmembrane domains. Sequence conservation between *Animalia* or *Vertebrata* is shown with asterisks for identical residues, colons for highly similar residues and periods for similar residues. (b) Details of sequence identity and similarity. (c) Cartoon of Pen-2 within the lipid membrane. (d) Human Pen-2 sequence including the N-terminal FLAG tag with residues mutated to alanine or other residues colored gray. Putative transmembrane domains are underlined.

In addition to facilitating PS endoproteolysis, Pen-2 can play other roles. The C-terminal region may be important for  $\gamma$ -secretase complex stability.<sup>19</sup> An endoplasmic retention signal sequence in TMD1 may be critical for trafficking.<sup>20</sup> Pen-2 is required for  $\gamma$ -secretase complex maturation in a manner independent of PS1 endoproteolysis as shown by a lack of Nct glycosylation in PS1 $\Delta$ Exon9 cells.<sup>21</sup> The N-terminal region may affect substrate processivity.<sup>22</sup> Adding to the complexity of this protein's function are two recent reports, one showing that purified PS1 holoprotein can undergo endoproteolysis upon addition of purified Pen-2 alone without a need for Aph1 or Nct<sup>23</sup> and the second using Pen-2 knockdown to propose that PS1 can undergo endoproteolysis without Pen-2.<sup>24</sup> Because of these multiple putative functions and little knowledge of the mechanisms by which this subunit acts upon  $\gamma$ -secretase, we have used a Pen-2 knockout cell line<sup>15</sup> to conduct an extensive mutagenesis screen to investigate Pen-2 cell localization, Pen-2 stability,  $\gamma$ -secretase activity, and  $\gamma$ -secretase maturation.

## EXPERIMENTAL PROCEDURES

**DNA Constructs.** All Pen-2 mutants were generated using the QuikChange Lightning Site-Directed Mutagenesis kit (Agilent Technologies) with primers designed by PrimerX (<http://www.bioinformatics.org/primerx>) and purchased from Life Technologies. The FLAG-Pen-2 template in pcDNA3.1(+)-Hygromycin was used as described previously.<sup>2</sup> C99 substrate came from a cDNA comprising the human APP signal sequence followed by the 99 C-terminal residues of human APP in pCAG (gift of T. Young-Pearse at the Center for Neurologic Diseases).

**Cell Lines and Transfection.** Pen-2 knockout mouse embryonic fibroblasts were a kind gift of B. De Strooper (KU Leuven, Leuven, Belgium). Cells were transfected using the 4D-Nucleofector X unit and P3 Primary Cell 4D-Nucleofector X kit (Lonza), recovered in RPMI medium with 10% FBS for 15 min, and then plated in 60 mm dishes with 4 mL of DMEM and 10% FBS. Six hours after the cells had been plated, media

were replaced with fresh DMEM and 10% FBS. Conditioned media were harvested after 18 h and stored at  $-80^{\circ}\text{C}$ . Cells were lysed in 1% CHAPSO, 50 mM HEPES (pH 7.2), 150 mM NaCl, and complete protease inhibitors (Roche). For each experiment, a set of several Pen-2 mutants was paired with wild-type Pen-2, and the same cell suspension was aliquoted and transiently transfected with each.

**Western Blotting, Enzyme-Linked Immunosorbent Assays (ELISAs), and Antibodies.** Western blot analyses were performed by electrophoreses of cell lysates on 4 to 12% Bis/Tris polyacrylamide gels, and the samples were transferred to polyvinylidene difluoride membranes and probed with the antibodies anti-human nicastrin (1:1000; BD Transduction Laboratories), anti-PS1-NTF (B19, kind gift of B. De Strooper), anti-PS1-CTF (1:2000; Abcam 76083), anti-Pen-2 (1:5000; Abcam 154830), anti-GAPDH (Novus Biologicals 221), anti-calnexin (1:2000; Abcam 22595), or anti- $\text{A}\beta$  (Calbiochem 6E10). All Western blots were scanned on an Odyssey Infrared Imaging System (Li-Cor), and densitometry analysis used Odyssey software.  $\text{A}\beta_{40}$  and  $\text{A}\beta_{42}$  from conditioned media were measured by triplex ELISA ( $\text{A}\beta$  capture by antibody 4G8) read on a Sector Imager 2400 (Mesoscale Discovery).

**Cell Surface Biotinylation.** Surface proteins were labeled using sulfo-NHS-SS-biotin (Thermo Scientific 21331) following the manufacturer's protocol. In brief, cells were grown to confluence and then washed gently four times with ice-cold PBS before the addition of 0.5 mg/mL sulfo-NHS-SS-biotin in PBS and incubation with shaking at room temperature for 30 min. Cross-linking was quenched by addition of Tris buffer (pH 8) to a final concentration of 50 mM and shaking for 10 min. Cells were washed four times with ice-cold PBS, then detached by being scraped in 25 mM EDTA in PBS buffer (pH 8), and pelleted at 16000g for 3 min at  $4^{\circ}\text{C}$ . Cell pellets were lysed in 1% CHAPSO, 50 mM HEPES (pH 7.2), 150 mM NaCl, and protease inhibitor cocktail (Roche) on ice for 1 h. Lysates were clarified by centrifugation at 21000g for 5 min and protein concentrations determined by the BCA assay (Thermo Scientific). Equal protein amounts were pulled down by mixing with streptavidin agarose in 0.2% CHAPSO and 0.08% digitonin in TBS at  $4^{\circ}\text{C}$  overnight. Unbound materials were removed, and resins were washed three times with ice-cold 0.1% digitonin in TBS before elution with Laemmli sample buffer and heating to  $65^{\circ}\text{C}$  for 5 min. Eluates and protein-normalized start lysates were subjected to 4 to 12% Bis/Tris sodium dodecyl sulfate-polyacrylamide gel electrophoresis (SDS-PAGE) for Western blotting.

**Pen-2 Stability Assay.** To measure Pen-2 and  $\gamma$ -secretase complex stability, fresh medium was added, and then cells were treated with a final concentration of 10  $\mu\text{M}$  MG132 or an equivalent volume of DMSO vehicle as a negative control at  $37^{\circ}\text{C}$  in 5%  $\text{CO}_2$  for 8 h. Cells were harvested and lysed as in the cell surface biotinylation experiments, and then equal protein amounts were resolved via SDS-PAGE for Western blotting.  $\beta$ -Catenin was used as a positive control to demonstrate proteasomal inhibition.<sup>25</sup>

**Immunoprecipitation (IP) Activity Assay.** IP activity assays were performed by immobilizing  $\gamma$ -secretase using anti-nicastrin (Sigma N1660) bound to protein A agarose at  $4^{\circ}\text{C}$  for 1.5 h, followed by three washes with 0.25% CHAPSO, 50 mM HEPES buffer (pH 7.2), and 150 mM NaCl. Resin was resuspended in 50  $\mu\text{L}$  of 1 mg/mL phosphatidylcholine, 0.25 mg/mL phosphatidylethanolamine, 0.25% CHAPSO [in 50 mM HEPES buffer (pH 7.2) and 150 mM NaCl], and 1  $\mu\text{M}$  C100-FLAG substrate<sup>26</sup> and incubated at  $37^{\circ}\text{C}$  for 3 h. Bound

samples were eluted with Laemmli sample buffer for analysis by SDS-PAGE and Western blotting, including resolution of various  $\text{A}\beta$  species on bicine/urea gels.<sup>9,12</sup> Quantification of bicine/urea Western blots was performed using ImageJ.

**Microsome Preparation.** Microsomes were prepared as described previously<sup>27</sup> with the addition of 10  $\mu\text{M}$  pepstatin A or vehicle (ethanol) at all stages of preparation.

**Statistics.** Statistical analysis of transient transfection Western blot densitometry and ELISA data were performed by the Harvard NeuroDiscovery Center's Biostatistics Consultation core. We fit mixed-effects models for the log of the ratio of  $\text{A}\beta_{40}$  from mutant Pen-2 to  $\text{A}\beta_{40}$  from wild-type Pen-2. This method included fixed effects for mutant Pen-2 and random effects for a date within a given mutant (to adjust for multiple samples for some mutants on some dates) and for a set within a date (to adjust for a particular wild-type sample). We apply a Bonferroni correction for the multiple testing due to the 39 mutants and use a *p* value threshold of  $0.05/39 = 0.001$ . Each mutant was tested on at least three independent occasions (*n* = 1–3 on each day) grouped with different mutants and compared to an internal wild-type control (*n* = 3–9). Statistical analysis of stable cell line experiments was performed using a one-way analysis of variance with Bonferroni correction to account for multiple comparisons with the wild-type control using GraphPad Prism. Cell surface biotinylation experimental data are the means of four independent experiments each with an *n* value of 1–3 (total *n* = 5–7).

## ■ RESULTS

Given the remarkable sequence conservation of the Pen-2 subunit of  $\gamma$ -secretase and its reported requirement for the maturation and catalytic activity of the complex, specific changes in the sequence may lead to alteration of specific functions. To test this hypothesis, key residues were mutated within Pen-2 (Figure 1d), and these mutant constructs were then expressed transiently to attempt to rescue a Pen-2 knockout mouse embryonic fibroblast (Pen-2 KO) line.<sup>15</sup> Effects of these mutants on complex maturation were analyzed by Western blot of cell lysates and densitometry. Proteolytic activities of the Pen-2 mutant-containing  $\gamma$ -complexes were examined by cotransfection of the transfected Pen-2 KO cells with human wild-type APP and subsequent ELISA analysis of  $\text{A}\beta$ .

Residues were chosen for mutation on the basis of a high degree of sequence conservation, the type of amino acid, and the location within the sequence. For example, the N-terminally clustered charged residues (E9, E10, and K11) were individually mutated to alanine. C15 was mutated to alanine and also to the more conservative serine to remove the thiol but minimally alter the polarity and size of the side chain. Conserved aromatic amino acids (particularly tryptophan and tyrosine) have affinity for the lipid polar headgroups and so can be largely found at the lipid–water interface important in defining the TMD boundaries.<sup>28</sup> Therefore, the conserved amino acids Y18, Y19, W36, F37, F38, and Y56 were each mutated to alanine to potentially disrupt the anchoring of TMDs to the lipid bilayer. Finally, P27 is located in the center of TMD1, and it would be predicted to induce a 30° bend in the helix.<sup>29</sup> Mutating this residue to alanine would remove this helix break and might potentially cause significant alterations in the incorporation and function of Pen-2 within  $\gamma$ -secretase.

**The Substrate Concentration Is Critical upon Cotransfection of Pen-2 KO MEFs with C99 and Pen-2.** Pen-2 KO MEFs<sup>15</sup> could be rescued with an N-terminally

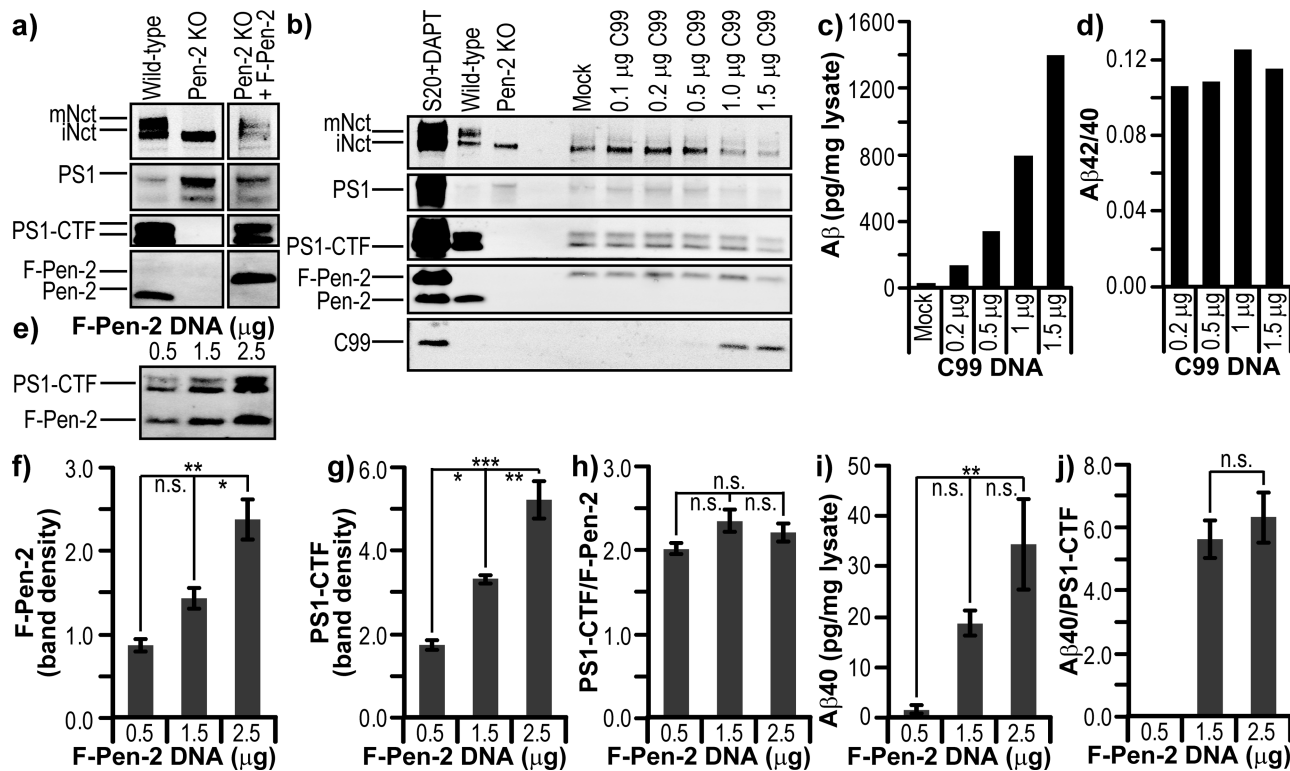


**Figure 2.** Validation of the Pen-2 KO MEF cell line. (a) Western blot comparing various components of  $\gamma$ -secretase in Pen-2 KO MEF cells with and without rescue using F-Pen-2, and MEF cells from wild-type littermates. (b) Western blot of Pen-2 KO cells rescued with 1.5  $\mu$ g of F-Pen-2 and cotransfected with increasing quantities of C99 DNA. CHO S20 cells, overexpressing all four  $\gamma$ -secretase components, treated with DAPT act as a control for C99 accumulation. (c) Secretion of A $\beta$  from cells measured by an ELISA and normalized to the total cell lysate. (d) Ratio of A $\beta$ <sub>42/40</sub> based on ELISA data. (e) Western blot of Pen-2 KO cells rescued with increasing quantities of F-Pen-2 DNA and cotransfected with 0.5  $\mu$ g of C99 DNA. (f) Densitometry of F-Pen-2 expression levels. (g) Densitometry of PS1-CTF levels. (h) Levels of PS1-CTF per unit of F-Pen-2. Levels of A $\beta$ <sub>40</sub> per (i) milligram of cell lysate and (j) unit of PS1-CTF. Error bars show the standard error from three replicates. \*P < 0.05. \*\*P < 0.01. \*\*\*P < 0.001.

FLAG-tagged wild-type (wt) Pen-2 (F-Pen-2), leading to complex maturation as shown by PS1 endoproteolysis (to NTF and CTF) and Nct maturation (further glycosylation) (Figure 2a). It should be noted that the addition of the FLAG tag retards migration of Pen-2 relative to the endogenous Pen-2 seen in MEFs from wt littermates (Figure 2a, left lane).

Before examining the effects of Pen-2 mutations on complex assembly, maturation, and activity, we sought to identify the factors needed for rescue of the Pen-2 KO cells and detection of substrate cleavage activity. With regard to  $\gamma$ -secretase activity, the level of secretion of A $\beta$  from Pen-2 KO cells rescued with wt F-Pen-2 was tested. Because of a very low level of endogenous expression of mouse APP in the cells, it was not possible to detect any A $\beta$  in conditioned media (data not shown). However, transfection of C99 with the APP signal sequence gave robust A $\beta$ <sub>40</sub> and A $\beta$ <sub>42</sub> secretion upon rescue with wt F-Pen-2. As a negative control, cells were also transfected with C99 in the absence of Pen-2 rescue and gave undetectable levels of A $\beta$  by an ELISA (data not shown).

To determine whether variability of substrate or active  $\gamma$ -secretase complexes could be tolerated for our analysis, Pen-2 KO cells were first transfected with a standard amount (1.5  $\mu$ g) of wt F-Pen-2 DNA and increasing amounts of C99 DNA. Equal expression levels of the  $\gamma$ -secretase components were seen regardless of the level of co-expressed C99 substrate (Figure 2b; because of cytotoxicity, the final two lanes have smaller amounts of total protein loaded). Normalization of A $\beta$  in the conditioned media to total cellular protein revealed a

stepwise increase in A $\beta$ <sub>40</sub> and A $\beta$ <sub>42</sub> production with an increasing level of C99 DNA (Figure 2c). A $\beta$ <sub>42/40</sub> ratios were consistently ~0.11–0.12 across all amounts of C99 DNA transfected (Figure 2d), a value that is squarely in the physiological range. In the reverse experiment, Pen-2 KO MEFs were then transfected with equal (0.5  $\mu$ g) amounts of C99 DNA and increasing amounts of wt F-Pen-2 DNA (Figure 2e), which revealed a stepwise increase in expression levels of F-Pen-2 (Figure 2f) and, as expected, of PS1-CTF (Figure 2g) as a measure of complex maturation. Figure 2h shows the ratio of PS1-CTF per unit of F-Pen-2, which is unchanging as the level of F-Pen-2 DNA increases. This relative uniformity is very important for the setup of all of our experiments (below), as it is likely that different mutants of Pen-2 may express to different degrees. Finally, we again see the expected stepwise increase in the level of A $\beta$  secretion with an increase in the level of wt F-Pen-2 DNA (Figure 2i), but when normalized to PS1-CTF (i.e., A $\beta$  per mature  $\gamma$ -secretase complex) levels of substrate cleavage do not vary (Figure 2j). Together, these experimental validation data inform us that it is essential for C99 expression levels to be equal between samples within a set of transfections, while a variable level of Pen-2 expression will not affect the analysis when normalizing to PS1-CTF.

To account for experiment-to-experiment variation in the expression levels of our different Pen-2 mutants (Figure 3b), internal controls were included to allow proper normalization. Each set of mutant F-Pen-2 transfections being performed on a given day also included one to three simultaneous wt F-Pen-2

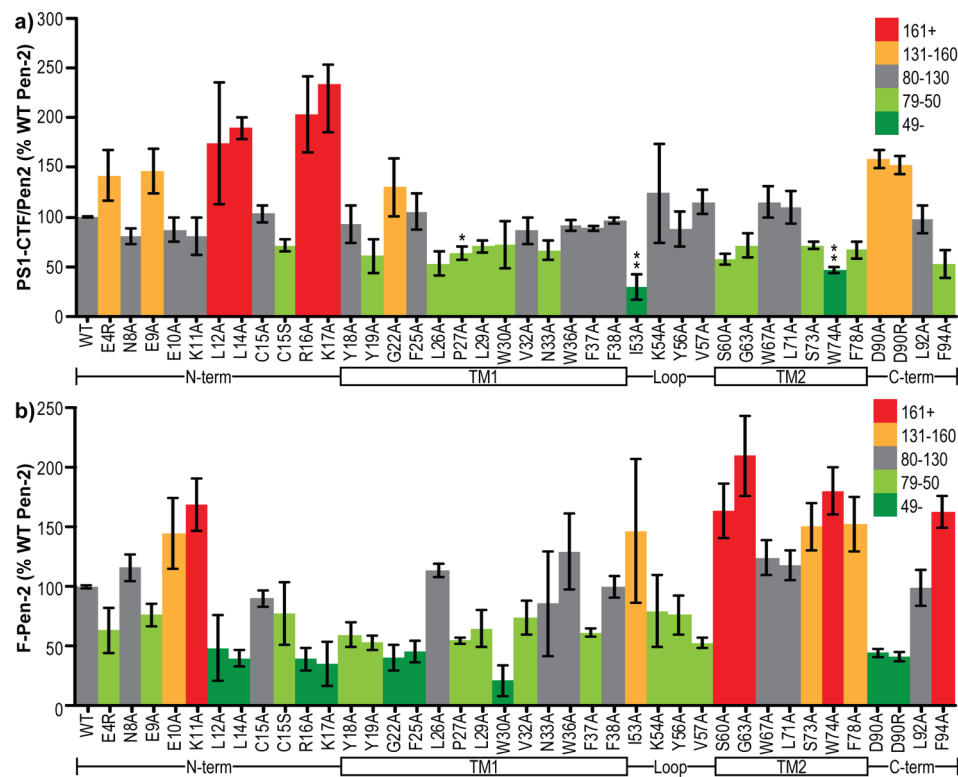


**Figure 3.** Pen-2 mutants rescue PS1 endoproteolysis to varying degrees. (a) Band intensity of PS1-CTF per unit of F-Pen-2 normalized to internal controls of wild-type human F-Pen-2. Colors denote the values above and below the wild-type value. (b) Band intensity of F-Pen-2 mutants normalized to internal controls of wild-type human F-Pen-2. Colors denote the values above and below the wild-type value. The schematic below each graph aligns the regions of Pen-2 being mutated. Error bars show the standard error from 3–10 independent experiments. \*P < 0.05. \*\*P < 0.01. \*\*\*P < 0.001.

control transfections. Values calculated within that experimental set were first normalized to total protein in the cell lysate and then expressed as a percentage of the mean wt F-Pen-2 value. Each data point shown is the mean of at least three independent experiments of one to three replicates, each normalized to their respective wt F-Pen-2 controls. To avoid data artifacts, the groupings of specific mutants transfected in a given experiment were varied between days.

**Pen-2 Mutants Rescue  $\gamma$ -Secretase Complex Maturation to Varying Degrees.** Unexpectedly, all of the Pen-2 mutants screened were able to at least partially rescue PS1 endoproteolysis. In the N-terminal region, E4R, E9A, L12A, L14A, R16A, and K17A all gave increases in the PS1-CTF:Pen-2 ratio relative to wt Pen-2 (Figure 3a). However, this may be misleading, as total Pen-2 levels (i.e.,  $\gamma$ -secretase-incorporated plus free) of those mutants were all below that of the wild type (Figure 3b), suggesting that rather than increasing the level of endoproteolysis, they reduce the stability of Pen-2, thus raising the relative ratio of PS1-CTF to Pen-2. In other words, transfection with these mutants leads to a degradation of unincorporated Pen-2 quicker than that with the wild type. In the case of C15S, a similar reduction in the total level of Pen-2 did not lead to an increase but rather a decrease in the level of PS1 endoproteolysis (Figure 3a), suggesting that this mutation is inefficient at supporting complex maturation. Most mutations within TMD1 led to a reduction in the total level of Pen-2, with W30A in particular at a level <20% of that of the wild type (Figure 3b). This is likely due to its decreased level of incorporation into  $\gamma$ -secretase, as shown by a reduced level of PS1 endoproteolysis (Figure 3a). Mutations within the loop

region generally reduced Pen-2 levels, with the exception of I53A, which had highly variable but somewhat elevated levels (Figure 3b). Of all mutants we tested, I53A caused the largest decrease in the level of PS1 endoproteolysis per Pen-2 unit, suggesting this site is particularly important in PS1 endoproteolysis (Figure 3a) because of either a weakened ability to allow endoproteolysis or a reduced affinity for  $\gamma$ -secretase. This question is addressed using stable cell lines, covered later in this study (Figures 7–9). Mutations in TMD2 almost all gave a large increase in total Pen-2 levels (Figure 3b) and in some cases a reduction in the level of PS1 endoproteolysis per Pen-2 (Figure 3a), suggesting an increase in the stability of unincorporated Pen-2. The same effect is found in the C-terminal region F94A mutation, while mutation of D90 to remove (>A) or reverse (>R) this negative charge substantially reduced the total level of Pen-2 (Figure 3b) and increased PS1-CTF:Pen-2 ratios (Figure 3a).

**Pen-2 Mutants Have Varying Effects on  $\gamma$ -Secretase Cleavage of the Substrate.** Via measurement of  $A\beta$  in media conditioned by Pen-2 KO cells cotransfected with C99 and mutant F-Pen-2 and normalization to PS1-CTF level (i.e., amount of  $A\beta$  produced per mature  $\gamma$ -secretase complex), the effect of mutations on substrate cleavage by  $\gamma$ -secretase can be determined. Surprisingly, several of the mutant Pen-2-containing  $\gamma$ -secretase complexes actually cleaved more substrate than wild-type Pen-2 complexes, while more than one-third caused a reduction in cleavage. Within the N-terminal region, the largest effects on  $\gamma$ -secretase cleavage activity were found with loss of the polar N8 residue, which increased  $A\beta_{40}$  to nearly 300% and  $A\beta_{42}$  to 180% of that of wt, and the L14A mutation, which increased  $A\beta_{40}$  to

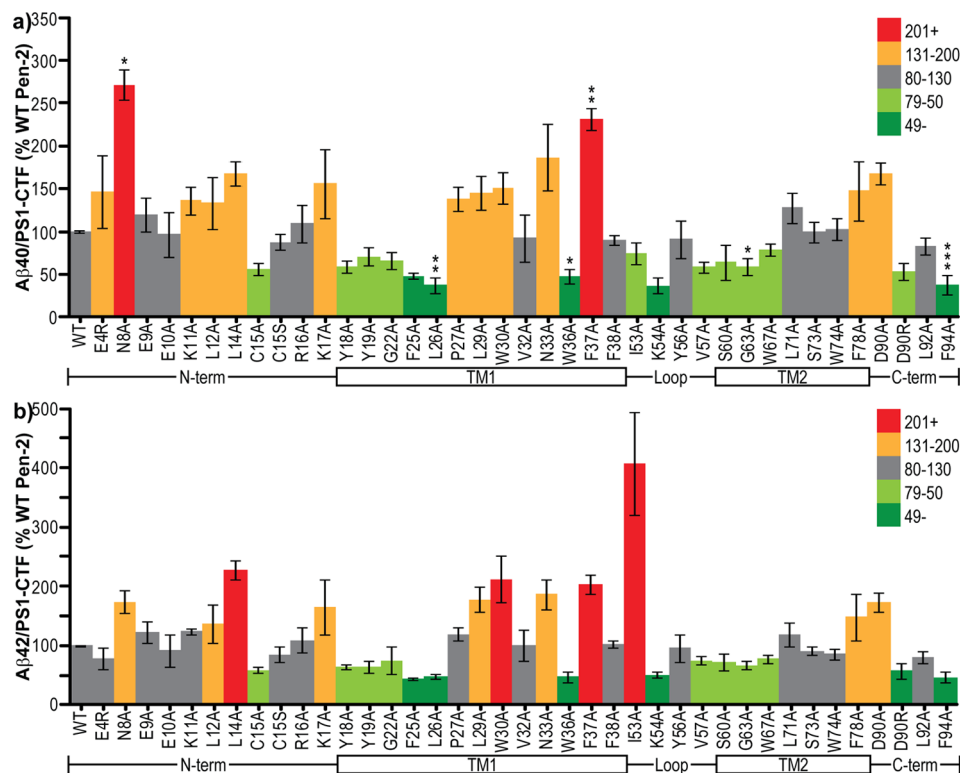


**Figure 4.**  $\gamma$ -Secretase activity levels per mature complex. (a)  $A\beta_{40}$  or (b)  $A\beta_{42}$  concentrations in conditioned media per unit of PS1-CTF normalized to internal controls of wt human F-Pen-2. Colors denote the values above and below the wild-type value. The schematic below each graph aligns the regions of Pen-2 being mutated. Error bars show the standard error from 3–10 independent experiments. \* $P < 0.05$ . \*\* $P < 0.01$ . \*\*\* $P < 0.001$ .

$\sim 160\%$  and  $A\beta_{42}$  to  $>200\%$  of that of wt (Figure 4a,b). The C15A mutation reduced both  $A\beta_{40}$  and  $A\beta_{42}$  to approximately 50%; however, the C15S mutation produced no change (Figure 4a,b). Mutation of either of the N-terminal positively charged (lysine) residues (K11 and K17) to alanine caused an increase in  $A\beta_{40}$  (Figure 4a) and in the case of K17 also increased  $A\beta_{42}$  (Figure 4b). All mutations within the top (N-terminal) half of TMD1 led to reduced  $A\beta_{40}$  and  $A\beta_{42}$  secretion, with the greatest effect from the bulky hydrophobic residues F25 and L26 (30–50% of that of wt) and a less pronounced effect in the cases of the two lipid–water interface aromatic residues Y18 and Y19 (70% of that of wt) (Figure 4a,b). Mutations in the lower (C-terminal) half of TMD1 had the opposite effect and elevated  $A\beta$  production, with the exception of the aromatic hydrogen bonding-capable W36, mutation of which lowered  $A\beta$  production. Interestingly, loss of the immediately adjacent aromatic hydrophobic F37 caused  $>2$ -fold increases in the production of both  $A\beta_{40}$  and  $A\beta_{42}$  (Figure 4a,b). Substantially enhanced cleavage was also caused by mutation of either the positively charged N33 or aromatic hydrophobic W30 to alanine (Figure 4a,b). Within the loop region, mutations I53A, V57A, and in particular K54A reduced  $A\beta_{40}$  secretion (Figure 4a). However,  $A\beta_{42}$  was very significantly increased in the case of I53A, while again the other mutants reduced cleavage (Figure 4b). Mutation of residues in TMD2 had relatively modest effects, with G63A/Y67A causing a slight decrease in both  $A\beta_{40}$  and  $A\beta_{42}$  and F78A causing a slight increase (Figure 4a,b). In the C-terminal region, a loss of the negatively charged D90 caused both  $A\beta_{40}$  and  $A\beta_{42}$  to increase to approximately 160% of that of wt, while reversing the charge to a positive arginine reduced secretion of both  $A\beta$  species to approximately half (Figure 4a,b). Finally, a loss of the

hydrophobic F94 led to a reduction in  $A\beta$  production to 40% of that of wt (Figure 4a,b).

**Effects on  $A\beta_{42/40}$  Ratios.** Of all the mutations tested, only a few had any effect on  $A\beta_{42/40}$  ratios, and those were relatively subtle. The one exception to this was with mutation of the hydrophobic I53, which caused a slight decrease in  $A\beta_{40}$  and a  $>4$ -fold increase in  $A\beta_{42}$ , thus leading to a doubling of the  $A\beta_{42/40}$  ratio (Figure 5). Other mutants causing a decrease in the ratio of  $A\beta$  species were mostly clustered in the lower half of TMD1 (i.e., including and right after the helix-breaking P27) but also occurred at the N-terminal region (E4R and N8A), upper TMD2 (S73A and W74A), and C-terminal D90A (Figure 5). The only other sites of mutation leading to elevated  $A\beta_{42/40}$  were two leucine residues (L14A and L26A) and a serine (S60A) (Figure 5).

#### Establishing Stable Cell Lines for Selected Mutants.

To further test the effect of some of the most interesting mutants of Pen-2, stable cell lines were established by stable transfection of Pen-2 KO MEF cells with wild-type, N8A, P27A, N33A, or I53A FLAG-Pen-2, with isolation of monoclonal cell lines. These lines were then screened for Pen-2 expression, and where possible, equally expressing lines were selected (Figure 6a,c). Levels of PS1-CTF generation per Pen-2 (Figure 6d) were similar to those observed in the transient transfections for N8A having little effect and P27A some reduction, while I53A decreased endoproteolysis but not as significantly. N33A caused a modest decrease in the PS1-CTF:Pen-2 ratio in the transient transfection experiments, but the stable line displayed elevated endoproteolysis (Figure 6d). However, upon IP via the FLAG tag of Pen-2, N8A, P27A, and N33A all displayed unaltered levels of  $\gamma$ -secretase maturation relative to that of wt Pen-2, but I53A showed  $<40\%$  wt levels of

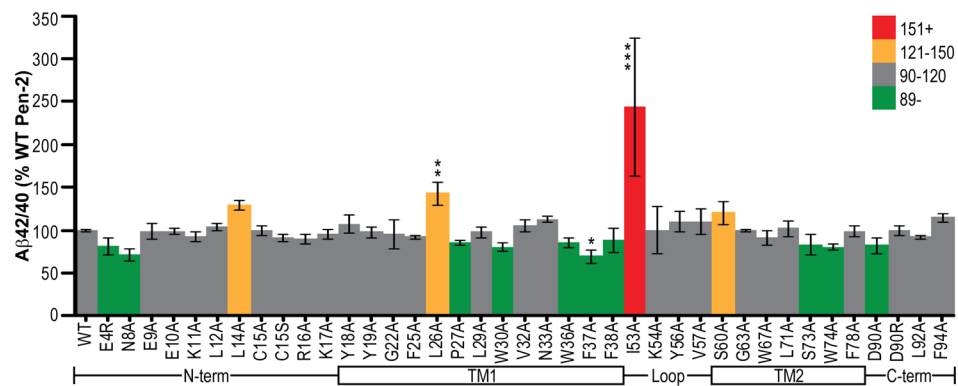


**Figure 5.** Effect of Pen-2 mutations on  $A\beta_{42/40}$  ratios. The  $A\beta_{42/40}$  ratio in conditioned media normalized to internal controls of wt human F-Pen-2. Colors denote the values above and below the wild-type value. The schematic below each graph aligns the regions of Pen-2 being mutated. Error bars show the standard error from 3–10 independent experiments. \* $P < 0.05$ . \*\* $P < 0.01$ . \*\*\* $P < 0.001$ .

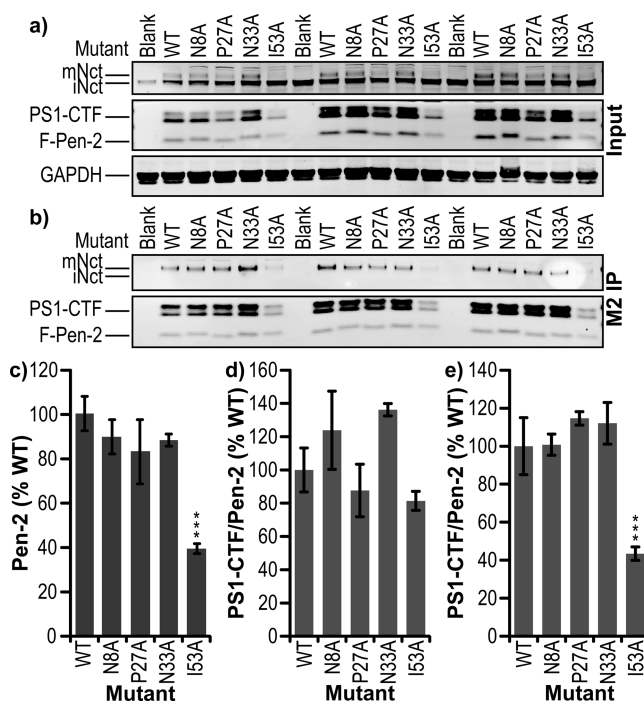


**Figure 6.** Stable cell lines of select Pen-2 mutants. Western blot of (a) total cell lysate (input) and (b) FLAG IP (M2 IP) of exogenous F-Pen-2 from monoclonal cell lines expressing wt, N8A, P27A, N33A, or I53A F-Pen-2. (c) Densitometric analysis of Pen-2 expression levels in each cell line normalized to internal controls of wild-type human F-Pen-2. (d) Band intensity of PS1-CTF per unit of F-Pen-2 normalized to internal controls of wild-type human F-Pen-2. (e) Band intensity of PS1-CTF per unit of F-Pen-2 immunoprecipitated via FLAG tag normalized to internal controls of wild-type human F-Pen-2. Error bars show the standard error from three independent experiments \* $P < 0.05$ . \*\* $P < 0.01$ . \*\*\* $P < 0.001$ .

PS1-CTF associated with Pen-2, suggesting an impaired complex stability (Figure 6b,e). Differences between transient transfections and stable cell lines data observed are likely due to the different mechanisms of expression in those two systems. The stable line has a more continuous but weaker expression, allowing an equilibrium of  $\gamma$ -complex incorporation and cell localization to be reached, while transient transfection by electroporation leads to an immediate high expression that may not be fully processed by cell machinery before the point of cell lysis. This is particularly apparent in the case of I53A, which in

the transient system had an apparent expression level approximately equal to that of wt (Figure 3b), while in the stable line, the value was <40% of wt (Figure 6c), in turn associating with 30% (Figure 3a) or 80% (Figure 6d) of wt PS1-CTF:Pen-2 levels. This temporary saturation of protein degradation machinery may also account for the discrepancy in the  $A\beta_{42/40}$  ratio between transient and stable transfactions with I53A Pen-2. In the transient system, I53A Pen-2 complexes may be able to initiate substrate cleavage but dissociate before full processing. N33A also showed a disparity between the transient and stable transfections for  $\gamma$ -secretase endoproteolysis, with the stable line having nearly 140% of the wt level in mature complexes per Pen-2 (Figure 6d) and the transient 70% (Figure 3a), but both with equal expression levels (Figures 3b and 6c). This may be due to the N33A complexes in the stable line having increased cell surface localization, which may be expected to elevate levels of the mature complex.

**Asn33 Is Involved in Pen-2 Localization within the Cell.** To examine the effect of certain mutations on the transport of Pen-2 and  $\gamma$ -secretase to the cell surface, where they are known to be active, we used the non-membrane permeable sulfo-NHS-SS-biotin to specifically label plasma membrane proteins via primary amines (i.e., lysine). The biotinylated proteins could then be specifically isolated from a total cell lysate using streptavidin agarose and then released by cleavage of the biotin–amine cross-link with  $\beta$ -mercaptoethanol. However, Pen-2 contains only two extracellular/luminal lysine residues (one of which forms the upper boundary of TMD1 and may not be fully accessible for cross-linking), so isolation of Pen-2 in NP40/RIPA buffer was very limited. This difficulty was overcome by lysing the cells in 1% CHAPSO/HEPES buffer and then pulling them down and washing them in 0.1% digitonin/HEPES buffer. Both of these detergents, in contrast with NP40, keep  $\gamma$ -secretase intact, allowing streptavidin pull-down via all biotinylated lysines in the intact  $\gamma$ -secretase complex. Digitonin is used for the binding and washing steps, as it removes weakly or nonspecifically interacting proteins. In these experiments, wild-type Pen-2 and its mutants could all be found at the cell surface in association with  $\gamma$ -secretase (Figure 7a). Surprisingly, PS1 holoprotein in the nonrescued Pen-2 KO line could also be biotinylated (data not shown), thus requiring confirmation that the biotinylation reagent had not passed the cell membrane by probing for the cytosolic protein GAPDH (Figure 7a). As a secondary control protein, the ER-associated transmembrane protein calnexin was also probed for; a small amount could be detected in the biotinylated/streptavidin

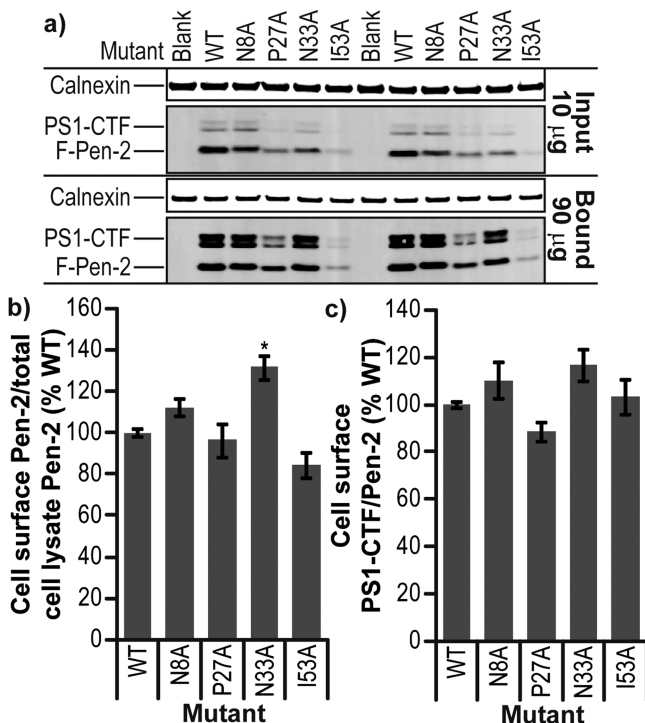


**Figure 7.** Effect of Pen-2 mutation on cell localization. (a) Western blot of 10  $\mu$ g of total cell lysate (Input) and 90  $\mu$ g of cell surface proteins pulled down with streptavidin agarose (Bound) for Pen-2 KO MEF cells rescued with mutants of Pen-2 and labeled with non-membrane permeable biotin. (b) Quantification of Pen-2 mutant levels at the cell surface compared to that of wild-type Pen-2. (c) Level of PS1-CTF per Pen-2 at the cell surface compared to that of wild-type Pen-2. Error bars show the standard error from three independent experiments. \* $P < 0.05$ . \*\* $P < 0.01$ . \*\*\* $P < 0.001$ .

pull-down sample ( $17 \pm 0.5$ -fold lower than the input lysate calnexin level), suggesting that up to 6% of our biotinylated sample could be from inside the cell (Figure 7a). This small amount of biotinylated calnexin could mean that the biotinylated PS1 holoprotein observed is not at the cell surface, rather in the endoplasmic reticulum within the cell. Measuring the ratio of cell surface mutant Pen-2 to that found in the lysate input and then normalizing to the ratio for wild-type Pen-2 revealed that among

the four mutants we studied in stable cell lines, only N33A showed a significant increase in the proportion of cell surface Pen-2 to total cellular Pen-2 (Figure 7b;  $P < 0.05$ ). Interestingly, this was not accompanied by an increase in PS1-CTF/Pen-2 (Figure 7c), as might be expected if more cell surface N33A Pen-2 is in mature  $\gamma$ -secretase.

**Ile53Ala and to a Lesser Extent Asn33Ala Reduce the Stability of Pen-2.** During the process of generating stable cell lines for some Pen-2 mutants, we noted that all clones of I53A had Pen-2 expression markedly lower than that of wild-type lines. Two possible reasons for this observation are (1) I53A Pen-2 is poorly expressed and (2) I53A Pen-2 has reduced affinity for PS1 and is targeted to the proteasome for degradation. We tested the second explanation by inhibiting the proteasome via treatment with MG132 (Figure 8a).  $\beta$ -Catenin, known to be degraded rapidly by the proteasome, served as a positive control. We found that wild-type Pen-2 and its four mutants rose to  $>200\%$  of untreated levels after MG132 treatment, with N33A and I53A increasing significantly more than wild type to 365 and almost 1000%, respectively ( $P < 0.001$ ) (Figure 8b). PS1-CTF levels increased correspondingly for wild-type and P27A, while N8A had an even greater elevation ( $P < 0.05$ ), resulting in a small but significant increase in the PS1-CTF:Pen-2 ratio ( $P < 0.01$ ). MG132 treatment of the N33A line did not significantly increase PS1-CTF, and there was therefore a slight decrease in its PS1-CTF:Pen-2 ratio ( $P < 0.01$ ). MG132 treatment of the I53A line caused PS1-CTF to increase by 400%, but because of the accompanying very large increase in Pen-2 levels, there was a very significant reduction in the PS1-CTF:Pen-2 ratio to 50% of that observed in wild-type cells treated with MG132 ( $P < 0.001$ ). These data show that the I53A mutation does not affect expression of Pen-2 but greatly reduces its stability because of enhanced proteasomal degradation. This MG132 treatment of the I53A line did not fully rescue the endoproteolysis of PS1, suggesting that this mutation may be affecting Pen-2 by reducing incorporation into and maturation and/or stability of  $\gamma$ -secretase.

**Mutating Pen-2 Does Not Affect  $\gamma$ -Secretase Processivity.** Given the striking increase in the  $A\beta_{42/40}$  ratio upon transient transfection of the I53A mutant into cells (Figure 5), an *in vitro*  $\gamma$ -secretase activity assay was used to cleave recombinant C100-FLAG, as is commonly used in cell-free  $\gamma$ -secretase assays.<sup>26,30</sup> Lysates of our stable cell lines were

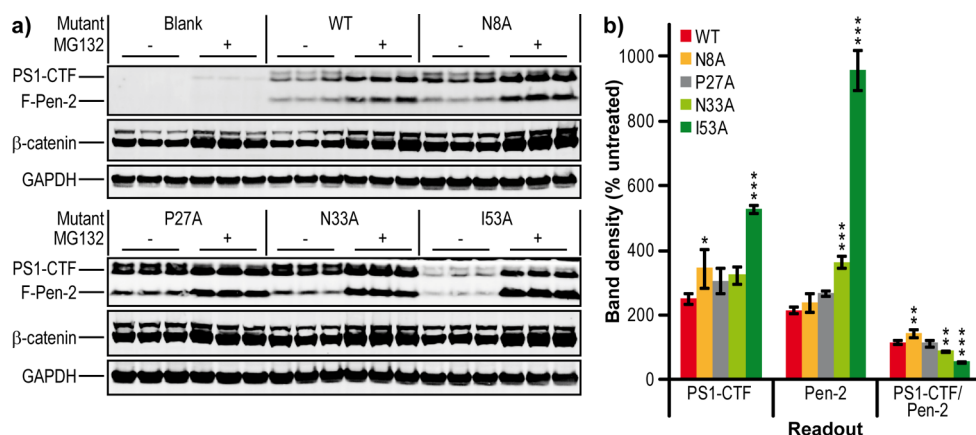


**Figure 8.** Effect of Pen-2 mutations on stability. (a) Western blot of total cell lysates for Pen-2 KO MEF cells rescued with mutants of Pen-2 and treated with 10  $\mu$ M MG132 or vehicle for 8 h. (b) Quantification of PS1-CTF and Pen-2 mutant levels and the amount of PS1-CTF per Pen-2 after MG132 treatment compared to that of a vehicle-treated sample. Bar colors denote wild-type and the four mutants tested. Error bars show the standard error from three replicates. \* $P < 0.05$ . \*\* $P < 0.01$ . \*\*\* $P < 0.001$ .

immunoprecipitated with anti-Nct antibodies, and on-bead activity assays were performed.  $\gamma$ -Secretase IP'ed from wt Pen-2 and all four mutant lines was able to cleave the C100-FLAG substrate, generating AICD-FLAG (Figure 9a); however, three

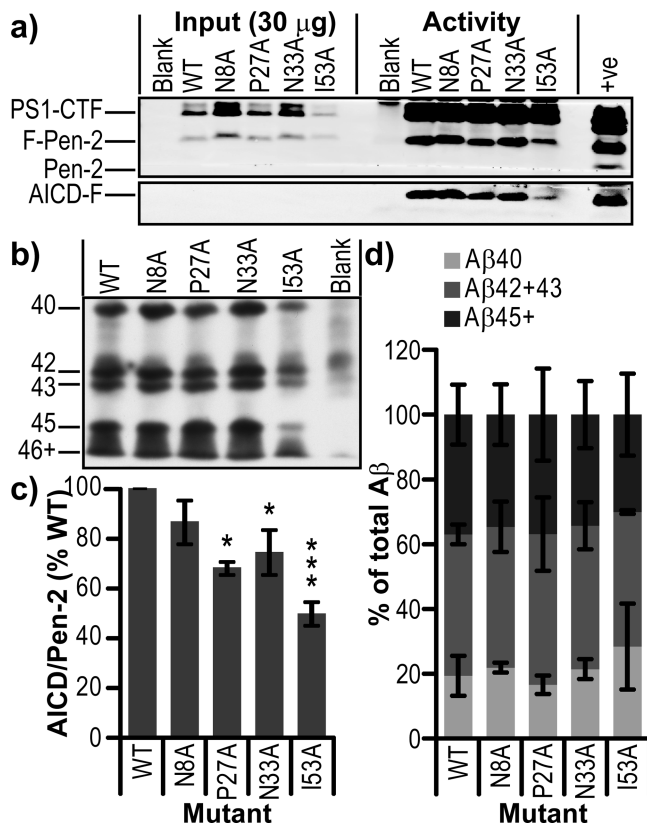


**Figure 9.** Effect of Pen-2 mutations on  $\gamma$ -secretase processivity. (a) Western blot of total cell lysate (Input) and IP activity assay (Activity) for Pen-2 KO MEF cells rescued with mutants of Pen-2. (b) Bicine/urea Western blot of IP activity assay supernatants. (c) Activity per mature  $\gamma$ -secretase complex calculated by densitometry of AICD-F/PS1-CTF. (d) Quantification of  $A\beta_{40}$ ,  $A\beta_{(42+43)}$ , and  $A\beta_{45+}$  displayed as a percentage of total  $A\beta$  in lane. Error bars show the standard error from two independent experiments. \* $P < 0.05$ . \*\* $P < 0.01$ . \*\*\* $P < 0.001$ .

mutants (P27A, N33A, and I53A) showed reduced activity upon normalization for Pen-2 levels (Figure 9c). The resultant  $A\beta$  peptides were then separated by bicine/urea polyacrylamide electrophoresis and detected by Western blotting (Figure 9b) and quantified by densitometry (Figure 9d). None of the mutants showed a significant difference from wt in the profile of  $A\beta$  peptides generated, suggesting that Pen-2 has no direct role in processivity.

**PS1 Endoproteolysis Is Possible in the Absence of Pen-2.** Over the course of the MG132 treatment experiments, we often noted what appeared to be background levels of PS1-CTF (Figure 8a) and PS1-NTF (not shown) in the Pen-2 KO MEFs. Treatment of Pen-2 KO cells with 10  $\mu$ M MG132 and harvesting at various time intervals revealed that PS1-CTFs accumulated over time (Figure 10a), albeit only to ~8% of wild-type MEF levels at the last time point [9 h (Figure 10b)]. To confirm that this observation is directly due to autoproteolysis of PS1 by the aspartic acid dyad, microsomes of Pen-2 KO cells were prepared in the presence of the aspartyl protease inhibitor pepstatin A (a known inhibitor of PS1 autoproteolysis<sup>31</sup>) or vehicle at all stages. In the absence of pepstatin A, accumulation of PS1-CTF and PS1-NTF was observed, with a

trace amount visible in the presence of inhibitor (Figure 10c). This endoproteolytic event occurred during the first step of cell lysis by homogenization but is not observed upon chemical lysis (data not shown). This result would suggest that the buffer condition (pH 6 MES buffer) and the membranes being in a vesicular form (no detergent) permit endoproteolysis, and protease inhibitors prevent degradation of the subsequent tripartite complex. Using immunoprecipitation of tripartite complexes via antibodies to Nct or PS1-CTF, it was possible to enrich the PS1 heterodimer from MG132-treated cell lysates and Pen-2 KO microsomes, but there was no detectable on-bead activity that could be measured by an AICD-FLAG Western blot or an  $A\beta_{40}$  ELISA (data not shown).

## DISCUSSION

Using a Pen-2 knockout mouse embryonic fibroblast cell line<sup>15</sup> rescued with Pen-2 constructs containing single missense mutations, we show that Pen-2 is intimately linked with both  $\gamma$ -secretase maturation and activity. Different regions and even individual amino acids within Pen-2 appear to have specific and important functions (summarized in Figure 11).

As the presenilin subunit of  $\gamma$ -secretase contains the catalytic aspartic acid residues and is the only subunit known to have familial Alzheimer's disease mutations, many studies have focused on this component. For example, using cysteine scanning approaches,<sup>32–35</sup> regions on several PS1 transmembrane domains have been identified to form part of a water-accessible pore, which is presumably the locus in which substrate hydrolysis occurs. It has even been proposed that PS1 can cleave the substrate in the absence of the three other  $\gamma$ -secretase components,<sup>23</sup> albeit at extremely low levels.

Considerable information is also available about nicastrin, partly because as the only  $\gamma$ -subunit with a large ectodomain, it may play a role in the recognition of the luminal end of a substrate or its access to the complex. The E333 residue of Nct has been reported to be required for  $\gamma$ -complex maturation<sup>36</sup> and possibly even activity.<sup>37</sup> On the other hand, some studies have suggested that Nct may be dispensable for  $\gamma$ -secretase activity.<sup>38,39</sup>

The other two components of  $\gamma$ -secretase have been rather less studied, with Aph1 suggested to act as a scaffold and thereby regulate assembly<sup>40</sup> and play a role in substrate docking,<sup>41</sup> and the Pen-2 subunit being necessary for PS endoproteolysis and subsequent stabilization of the mature, active complex.<sup>4,19</sup>

Because of the high level of sequence identity of Pen-2 between different species and its invariable length of 101 amino acids, we systematically mutated numerous residues within different regions of the protein and examined the effect on  $\gamma$ -secretase maturation and activity. Surprisingly, none of the mutants tested completely abrogated either complex maturation (i.e., PS endoproteolysis) or activity. This result is in agreement with a scanning cysteine mutagenesis study.<sup>15</sup> This lack of complete loss of function in the two studies may relate to mutating only single residues rather than clusters. For example, mutation of D90YLSF to pentaalanine prevented the association of Pen-2 with other components of  $\gamma$ -secretase and hence PS1 endoproteolysis.<sup>42</sup> Similarly, mutation of four nonadjacent residues near the C-terminus to alanine caused complex maturation to be completely halted.<sup>19</sup> However, when we tested a cluster mutation of N8EE>AAA, PS1 endoproteolysis appeared unaffected while  $A\beta$  production per  $\gamma$ -secretase complex was elevated approximately 3-fold above that of wild-type Pen-2 (data not shown). These results indicate that different regions of Pen-2 have different roles in  $\gamma$ -secretase function.

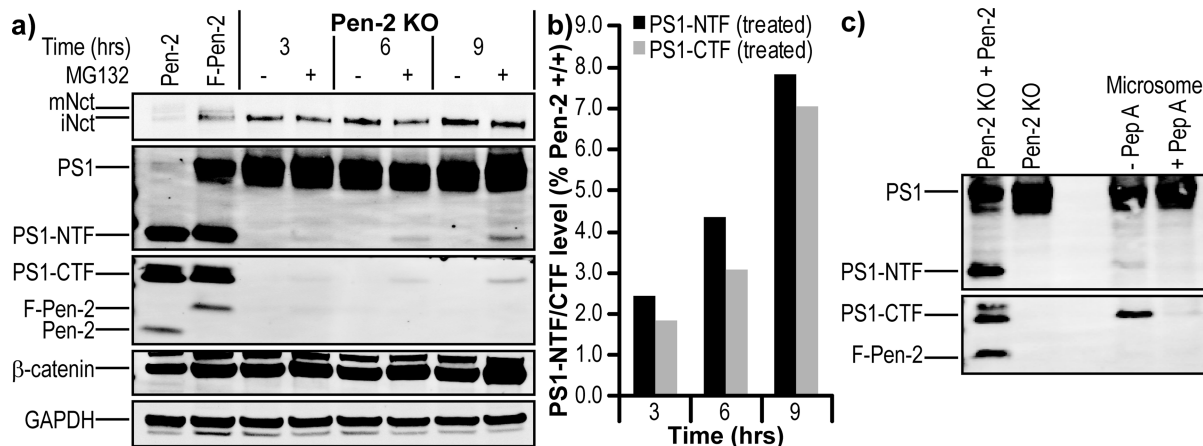


**Figure 10.** PS1 can undergo endoproteolysis in the absence of Pen-2. (a) Western blot and (b) quantification showing a time course of Pen-2 KO MEF cell treatment with 10  $\mu$ M MG132 or vehicle. (c) Western blot of microsomes prepared from Pen-2 KO MEF cells in the absence or presence of 10  $\mu$ M pepstatin A. The left two lanes contained lysates of Pen-2 KO rescued with F-Pen-2 or without rescue.

With the exceptions of E10A, K11A, and W36A mutations, mutation of most residues in the N-terminal region and in TMD1 reduced Pen-2 expression. Altering the amino acid sequence in this region could change the initial fold and entry of TMD1 into the membrane, which in turn may cause the protein to be targeted to the proteasome for degradation. In the case of W30A, where a dramatic (20% of the wt level) loss of expression was seen, the loss of a bulky hydrophobic residue in the center of the transmembrane domain appears to be detrimental. Interestingly, the K11A mutant has approximately 170% of wt expression levels, which could mean this is a normal ubiquitination site (despite being on the luminal side of the membrane). Bergman et al.<sup>43</sup> reported that mutation of the sole cytosolic lysine residue, K54, to R did not prevent ubiquitination of Pen-2. These authors also assessed a Pen-2 with all three lysines mutated to arginine, but the protein could not be expressed. Here, we found that K54A and K17A mutations had little effect on Pen-2 expression. This result would leave K11 as a candidate for the ubiquitination target, although we cannot exclude ubiquitination of non-lysine sites such as serine/threonine.<sup>44,45</sup> In this regard, we obtained 170% of wt Pen-2 levels with the S60A mutant. Similar increases in Pen-2 levels were also found with most mutations in TMD2, suggesting a previously unrecognized role of TMD2 in the stability of Pen-2.

Mutation of several residues in the N-terminal region, especially N8A and L14A, also caused an elevation in substrate cleavage. This could be due to loss of an interaction with a luminal region of PS1, thus altering active site conformation, or the fact that these residues normally block the entry of the substrate into the active site.

In addition to their reducing Pen-2 levels, almost all mutants in TMD1 (from Y19 to N33) produced a decrease in PS1-CTF per Pen-2 to 50–70% of the wt value. This agrees with a prior report that the upper two-thirds of TMD1 is necessary for PS1 endoproteolysis.<sup>18</sup> Two independent reports used domain swapping of TMDs within PS1 to narrow the Pen-2 binding site to a W203NF motif in the center of PS1 TMD4.<sup>17,46</sup> Mutations in the upper half of Pen-2 TMD1 may be partly deficient in their ability to initiate endoproteolysis because of a change in the conformation of the active site in PS1. Following the same line of reasoning, without exception all mutants tested in TMD1 above P27 caused a reduction in  $\text{A}\beta$  generated per mature  $\gamma$ -secretase complex to 55–70% of wt levels.

Mutation of most residues from P27 to the end of TMD1 elevated substrate cleavage, producing 140–230% of the wt level of  $\text{A}\beta_{40}$  and  $\text{A}\beta_{42}$  and in some cases a modest decrease in the  $\text{A}\beta_{42/40}$  ratio. These substitutions on Pen-2 all replace a large side chain with the small methyl group of alanine, perhaps allowing PS1 to expand into a more open conformation previously shown to lead to a relative decrease in  $\text{A}\beta_{42}$ <sup>47</sup> and an increase in substrate access to the active site. The exception in this region was the W36A mutant, which led to a 50% level in both  $\text{A}\beta$  species, possibly due to a change in the anchoring of the bottom of TMD1 with the lipid–water interface and thereby allowing F37/38 to form part of the transmembrane domain. Mutation of F37 to alanine had the opposite effect, raising  $\text{A}\beta$  secretion to >200% compared to the wt value.

Our mutations in TMD2 mostly decreased the PS1-CTF:Pen-2 ratio, primarily because of increases in Pen-2. This may represent excess free Pen-2 resulting from deficient degradation of the mutants, perhaps due to their altered cellular localization. In this regard, N33 in TMD1 of Pen-2 was found to be targeted by the ER retention protein Rer1,<sup>20</sup> and a report that the WNF motif in PS1 TMD4 is also a Rer1 binding site<sup>48</sup> led to the proposal of a masking of ER retention signals upon binding of Pen-2 to PS1 concealed both their Rer1 binding sites, allowing  $\gamma$ -secretase to move to the Golgi apparatus. Our cell surface labeling experiments indeed confirm that N33 is involved in preventing Pen-2 from moving to the plasma membrane. However, we saw an equal increase in PS1-CTF at the cell surface of the N33A Pen-2 cells, implying proper localization of the mature complex rather than mislocalization of free Pen-2, thus arguing against the masking hypothesis. A possible explanation for this discrepancy could be that as we detected trace amounts of the ER-associated protein calnexin, we may have inadvertently also labeled some PS1-CTF within the cell, thus masking a potential slightly lower level of PS1-CTF at the cell surface, which would then argue for N33A Pen-2 shifting to the plasma membrane independently of the rest of the  $\gamma$ -secretase complex. Mutation of residues in the lower half of TMD2 may decrease  $\text{A}\beta$  production by altering the initial fold of this TMD, thus changing the alignment of the rest of the TMD. No other mutations we made in TMD2 affected substrate cleavage, and given its somewhat lower level of sequence conservation, this domain may simply be required to position the C-terminal domain relative to the rest of Pen-2.

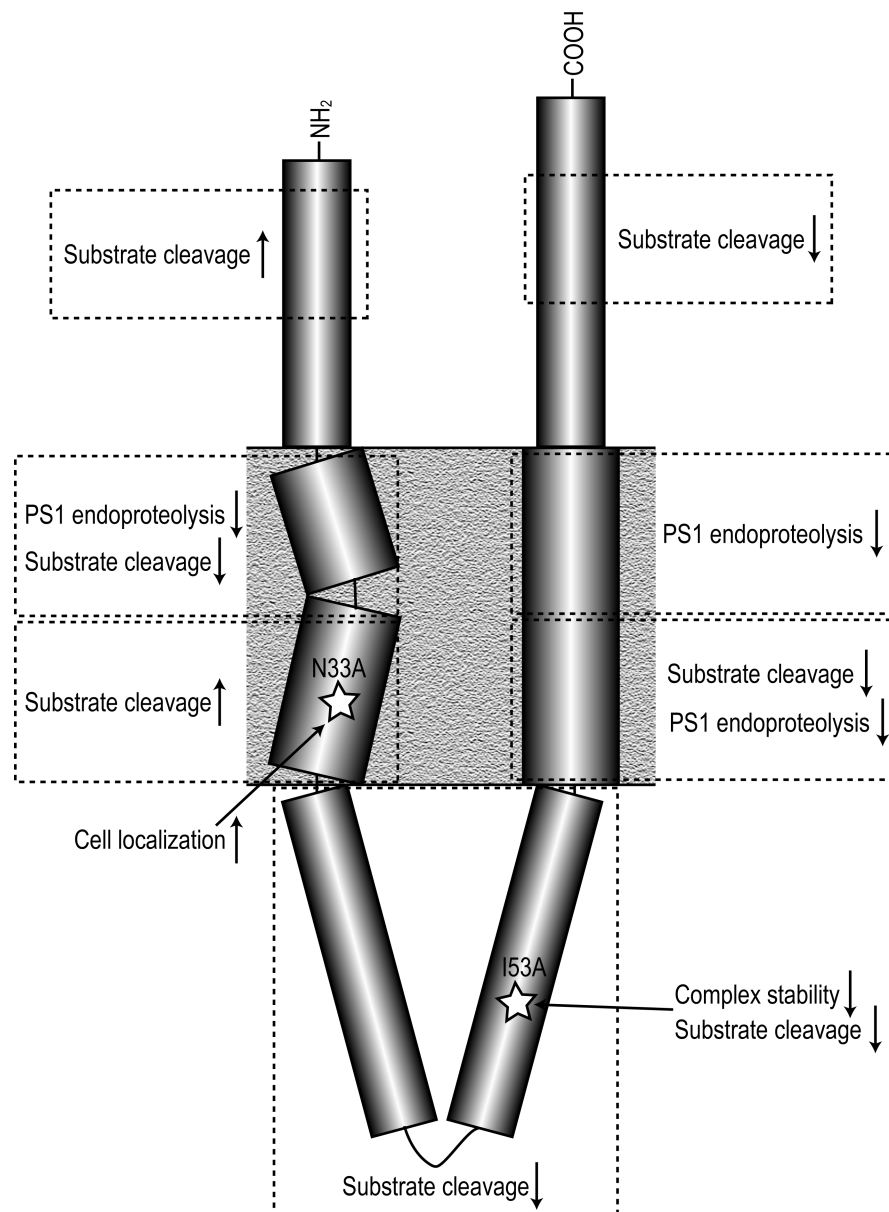


**Figure 11.** Effect of mutation of different regions of Pen-2. Cartoon summarizing the effect of mutation of regions of the Pen-2 subunit on  $\gamma$ -secretase PS1 endoproteolysis, substrate cleavage, complex stability, and cell localization.

As with TMD2, mutations in the C-terminus led to changes in PS1-CTF/Pen-2 that seemed to correlate with Pen-2 expression levels. This appears to be at odds with a report that point mutations to alanine within the C-terminus had no effect on Pen-2 expression or PS1 endoproteolysis, although simultaneous mutation of all four fully conserved residues (D90, F94, P97, and G99) decreased the stability of the  $\gamma$ -complex.<sup>19</sup> This apparent discrepancy may relate to their use of stable Pen-2 shRNA expression, so that some endogenous Pen-2 and corresponding low-level PS1 endoproteolysis remain (vs full knockout of Pen-2 here). Another difference is that the study by Prokop et al. used stable cell lines for each mutant, while we used transient transfections. Although a previous report<sup>42</sup> found that mutation of some residues within the D90YLSF motif of Pen-2 to alanine decreased  $A\beta$  production during Pen-2 knockdown rescue, we found the opposite effect with D90A, a 70% increase in  $A\beta$ . This difference is likely to be due to our calculating  $A\beta$  production per mature  $\gamma$ -secretase

complex, while the study by Hasegawa et al. showed raw  $A\beta$  per milligram of protein values despite a level of PS1-NTF clearly lower than that with wild-type Pen-2. Interestingly, when D90 is changed conservatively to E, a near-wild-type level of PS1 endoproteolysis occurs but  $A\beta$  generation is still reduced, albeit less than with the D90A mutant. We also found that reversing the charge (D90R) halved  $\gamma$ -activity. Mutation of the highly conserved F94 to alanine caused a significant decrease in  $A\beta$  production.

Finally, we found two sites of particular interest in the cytosolic loop region. K54A had no effect on expression or endoproteolysis, as previously shown by Bammens et al.,<sup>15</sup> but did cause reductions to 40 and 50% of wt levels for  $A\beta_{40}$  and  $A\beta_{42}$ , respectively. When stably expressed, the adjacent I53A mutation showed a reduction in stability but was still able to partially support endoproteolysis, which could be further rescued by inhibition of the proteasome. However, the increase in endoproteolysis was substantially smaller than would be

expected if corresponding directly to Pen-2 levels, indicating that the I53A Pen-2  $\gamma$ -complexes have reduced stability. In addition to the reduced complex stability, each intact complex also displayed a 50% level of substrate cleavage *in vitro*. Together, these novel data indicate that this isoleucine residue is very important for the overall stability and function of  $\gamma$ -secretase. This finding leads us to hypothesize that the cytosolic loop region of Pen-2 may be directly and critically interacting with PS1. Given the location of this region and the previous reports of Pen-2 TMD1 to PS1 TMD4<sup>17,46</sup> and TMD2 binding to PS1-CTF,<sup>15</sup> a possible candidate for Pen-2 I53 binding is to the conserved hydrophobic domain VII (HDVII) of the large loop region of PS1. The short Pen-2 loop region could then bring the large PS1 cytosolic loop closer to the catalytic core, allowing subsequent autoproteolysis.

During the proteasome inhibition experiments, we observed a faint signal for PS1-NTF/CTF in plain Pen-2 KO cell lysates. This curious observation was also reported by Mao et al.,<sup>24</sup> although they used Pen-2 siRNA, which may leave trace levels of Pen-2. Thus, our experiments in Pen-2 knockout cells now confirm the report by Mao et al. We find that endoproteolysis appears to be facilitated under mildly acidic conditions that coincide with the pH found in the Golgi network,<sup>49</sup> the initial site of  $\gamma$ -secretase complex maturation<sup>31</sup> and the first site of detectable APP cleavage.<sup>50</sup> It is still possible that this cleavage is occurring due to another protease, but given that it can be inhibited by pepstatin A, this would specifically necessitate an aspartyl protease capable of cleaving at or very close to the endoproteolytic site of  $\gamma$ -secretase, which would seem to be an unlikely combination. Ahn et al. previously reported that PS1  $\Delta E9$  is able to cleave the substrate in the absence of any other  $\gamma$ -secretase subunits.<sup>23</sup> Using both Pen-2 KO microsomes and Pen-2 KO MG132-treated lysate IPs, we detected no substrate cleavage measured by an AICD-FLAG Western blot or an  $A\beta_{40}$  ELISA. By comparing PS1-CTF band intensity for wt Pen-2 (Figure 9a) and MG132-treated Pen-2 KO (data not shown) IP activity assays, we would expect a 5–10% level of cleavage. This would equate to  $A\beta_{40}$  production in the range of 50–200 pg/mL, which is within the detection limits of our ELISA. We therefore suggest that PS1 heterodimer–Nct–Aph1 tripartite complexes are either inactive or only partially active. Pen-2 binding to PS1 may act to stabilize these complexes, allowing time for autoproteolysis and activation to occur. The relatively less stable PS1 heterodimer can then be held together by interactions of Pen-2 TMD1 with PS1 TMD4, Pen-2 loop with PS1 HDVII, and Pen-2 TMD2 with PS1-CTF.

In summary, we use systematic mutagenesis to provide evidence that the mechanism by which Pen-2 functions in the context of  $\gamma$ -secretase is multivariate, with different regions and even individual residues having apparently different roles. We also observed apparent PS1 endoproteolysis in the complete absence of Pen-2. An improved understanding of these mechanisms may require detailed structural information about the nature of the Pen-2–PS1 interaction.

## ■ AUTHOR INFORMATION

### Corresponding Author

\*Brigham and Women's Hospital, 77 Avenue Louis Pasteur, H.I.M. 754, Boston, MA 02115. E-mail: mwolfe@rics.bwh.harvard.edu. Telephone: (617) 525-5511. Fax: (617) 525-5252.

### Funding

This work was supported by National Institutes of Health Grant P01 AG015379.

### Notes

The authors declare no competing financial interest.

## ■ ACKNOWLEDGMENTS

We thank Bart De Strooper for providing the Pen-2 knockout MEF cell line.

## ■ ABBREVIATIONS

AD, Alzheimer's disease; APP,  $\beta$ -amyloid precursor protein;  $A\beta$ , amyloid  $\beta$ -peptide; AICD, APP intracellular domain; CHAPSO, 3-[[(3-cholamidopropyl)dimethylammonio]-2-hydroxy-1-propanesulfonic acid; MEF, mouse embryonic fibroblast; PS, presenilin; TMD, transmembrane domain.

## ■ REFERENCES

- (1) Wolfe, M. S., Xia, W., Ostaszewski, B. L., Diehl, T. S., Kimberly, W. T., and Selkoe, D. J. (1999) Two transmembrane aspartates in presenilin-1 required for presenilin endoproteolysis and  $\gamma$ -secretase activity. *Nature* 398, 513–517.
- (2) Kimberly, W. T., LaVoie, M. J., Ostaszewski, B. L., Ye, W., Wolfe, M. S., and Selkoe, D. J. (2003)  $\gamma$ -Secretase is a membrane protein complex comprised of presenilin, nicastrin, Aph-1, and Pen-2. *Proc. Natl. Acad. Sci. U.S.A.* 100, 6382–6387.
- (3) Elbauer, D., Winkler, E., Regula, J. T., Pesold, B., Steiner, H., and Haass, C. (2003) Reconstitution of  $\gamma$ -secretase activity. *Nat. Cell Biol.* 5, 486–488.
- (4) Takasugi, N., Tomita, T., Hayashi, I., Tsuruoka, M., Niimura, M., Takahashi, Y., Thinakaran, G., and Iwatsubo, T. (2003) The role of presenilin cofactors in the  $\gamma$ -secretase complex. *Nature* 422, 438–441.
- (5) Brown, M. S., Ye, J., Rawson, R. B., and Goldstein, J. L. (2000) Regulated intramembrane proteolysis: A control mechanism conserved from bacteria to humans. *Cell* 100, 391–398.
- (6) Kopan, R., and Ilagan, M. X. (2004)  $\gamma$ -Secretase: Proteasome of the membrane? *Nat. Rev. Mol. Cell Biol.* 5, 499–504.
- (7) Weidemann, A., Eggert, S., Reinhard, F. B., Vogel, M., Paliga, K., Baier, G., Masters, C. L., Beyreuther, K., and Evin, G. (2002) A novel  $\epsilon$ -cleavage within the transmembrane domain of the Alzheimer amyloid precursor protein demonstrates homology with Notch processing. *Biochemistry* 41, 2825–2835.
- (8) Gu, Y., Misonou, H., Sato, T., Dohmae, N., Takio, K., and Ihara, Y. (2001) Distinct intramembrane cleavage of the  $\beta$ -amyloid precursor protein family resembling  $\gamma$ -secretase-like cleavage of Notch. *J. Biol. Chem.* 276, 35235–35238.
- (9) Takami, M., Nagashima, Y., Sano, Y., Ishihara, S., Morishima-Kawashima, M., Funamoto, S., and Ihara, Y. (2009)  $\gamma$ -Secretase: Successive tripeptide and tetrapeptide release from the transmembrane domain of  $\beta$ -carboxyl terminal fragment. *J. Neurosci.* 29, 13042–13052.
- (10) Pauwels, K., Williams, T. L., Morris, K. L., Jonckheere, W., Vandersteen, A., Kelly, G., Schymkowitz, J., Rousseau, F., Pastore, A., Serpell, L. C., and Broersen, K. (2012) Structural basis for increased toxicity of pathological  $A\beta42:A\beta40$  ratios in Alzheimer disease. *J. Biol. Chem.* 287, 5650–5660.
- (11) Saito, T., Suemoto, T., Brouwers, N., Sleegers, K., Funamoto, S., Miura, N., Matsuba, Y., Yamada, K., Nilsson, P., Takano, J., Nishimura, M., Iwata, N., Van Broeckhoven, C., Ihara, Y., and Saido, T. C. (2011) Potent amyloidogenicity and pathogenicity of  $A\beta43$ . *Nat. Neurosci.* 14, 1023–1032.
- (12) Quintero-Monzon, O., Martin, M. M., Fernandez, M. A., Cappello, C. A., Krzysiak, A. J., Osenkowski, P., and Wolfe, M. S. (2011) Dissociation between the processivity and total activity of  $\gamma$ -secretase: Implications for the mechanism of Alzheimer's disease-causing presenilin mutations. *Biochemistry* 50, 9023–9035.
- (13) Fukumori, A., Fluhrer, R., Steiner, H., and Haass, C. (2010) Three-amino acid spacing of presenilin endoproteolysis suggests a general stepwise cleavage of  $\gamma$ -secretase-mediated intramembrane proteolysis. *J. Neurosci.* 30, 7853–7862.

- (14) Thinakaran, G., Borchelt, D. R., Lee, M. K., Slunt, H. H., Spitzer, L., Kim, G., Ratovitsky, T., Davenport, F., Nordstedt, C., Seeger, M., Hardy, J., Levey, A. I., Gandy, S. E., Jenkins, N. A., Copeland, N. G., Price, D. L., and Sisodia, S. S. (1996) Endoproteolysis of presenilin 1 and accumulation of processed derivatives in vivo. *Neuron* 17, 181–190.
- (15) Bammens, L., Chavez-Gutierrez, L., Tolia, A., Zwijsen, A., and De Strooper, B. (2011) Functional and topological analysis of Pen-2, the fourth subunit of the  $\gamma$ -secretase complex. *J. Biol. Chem.* 286, 12271–12282.
- (16) Crystal, A. S., Morais, V. A., Pierson, T. C., Pijak, D. S., Carlin, D., Lee, V. M., and Doms, R. W. (2003) Membrane topology of  $\gamma$ -secretase component PEN-2. *J. Biol. Chem.* 278, 20117–20123.
- (17) Watanabe, N., Tomita, T., Sato, C., Kitamura, T., Morohashi, Y., and Iwatsubo, T. (2005) Pen-2 is incorporated into the  $\gamma$ -secretase complex through binding to transmembrane domain 4 of presenilin 1. *J. Biol. Chem.* 280, 41967–41975.
- (18) Kim, S. H., and Sisodia, S. S. (2005) A sequence within the first transmembrane domain of PEN-2 is critical for PEN-2-mediated endoproteolysis of presenilin 1. *J. Biol. Chem.* 280, 1992–2001.
- (19) Prokop, S., Haass, C., and Steiner, H. (2005) Length and overall sequence of the PEN-2 C-terminal domain determines its function in the stabilization of presenilin fragments. *J. Neurochem.* 94, 57–62.
- (20) Kaether, C., Scheuermann, J., Fassler, M., Zilow, S., Shirotani, K., Valkova, C., Novak, B., Kacmar, S., Steiner, H., and Haass, C. (2007) Endoplasmic reticulum retention of the  $\gamma$ -secretase complex component Pen2 by Rer1. *EMBO Rep.* 8, 743–748.
- (21) Prokop, S., Shirotani, K., Edbauer, D., Haass, C., and Steiner, H. (2004) Requirement of PEN-2 for stabilization of the presenilin N-/C-terminal fragment heterodimer within the  $\gamma$ -secretase complex. *J. Biol. Chem.* 279, 23255–23261.
- (22) Isoo, N., Sato, C., Miyashita, H., Shinohara, M., Takasugi, N., Morohashi, Y., Tsuji, S., Tomita, T., and Iwatsubo, T. (2007)  $\text{A}\beta42$  overproduction associated with structural changes in the catalytic pore of  $\gamma$ -secretase: Common effects of Pen-2 N-terminal elongation and fenofibrate. *J. Biol. Chem.* 282, 12388–12396.
- (23) Ahn, K., Shelton, C. C., Tian, Y., Zhang, X., Gilchrist, M. L., Sisodia, S. S., and Li, Y. M. (2010) Activation and intrinsic  $\gamma$ -secretase activity of presenilin 1. *Proc. Natl. Acad. Sci. U.S.A.* 107, 21435–21440.
- (24) Mao, G., Cui, M. Z., Li, T., Jin, Y., and Xu, X. (2012) Pen-2 is dispensable for endoproteolysis of presenilin 1, and nicastrin-Aph subcomplex is important for both  $\gamma$ -secretase assembly and substrate recruitment. *J. Neurochem.* 123, 837–844.
- (25) Ghanevati, M., and Miller, C. A. (2005) Phospho- $\beta$ -catenin accumulation in Alzheimer's disease and in aggresomes attributable to proteasome dysfunction. *J. Mol. Neurosci.* 25, 79–94.
- (26) Li, Y. M., Lai, M. T., Xu, M., Huang, Q., DiMuzio-Mower, J., Sardana, M. K., Shi, X. P., Yin, K. C., Shafer, J. A., and Gardell, S. J. (2000) Presenilin 1 is linked with  $\gamma$ -secretase activity in the detergent solubilized state. *Proc. Natl. Acad. Sci. U.S.A.* 97, 6138–6143.
- (27) Fraering, P. C., Ye, W., Strub, J. M., Dolios, G., LaVoie, M. J., Ostaszewski, B. L., van Dorsselaer, A., Wang, R., Selkoe, D. J., and Wolfe, M. S. (2004) Purification and characterization of the human  $\gamma$ -secretase complex. *Biochemistry* 43, 9774–9789.
- (28) Killian, J. A., and von Heijne, G. (2000) How proteins adapt to a membrane-water interface. *Trends Biochem. Sci.* 25, 429–434.
- (29) Richardson, J. S. (1981) The anatomy and taxonomy of protein structure. *Adv. Protein Chem.* 34, 167–339.
- (30) Kimberly, W. T., Esler, W. P., Ye, W., Ostaszewski, B. L., Gao, J., Diehl, T., Selkoe, D. J., and Wolfe, M. S. (2003) Notch and the amyloid precursor protein are cleaved by similar  $\gamma$ -secretase(s). *Biochemistry* 42, 137–144.
- (31) Campbell, W. A., Reed, M. L., Strahle, J., Wolfe, M. S., and Xia, W. (2003) Presenilin endoproteolysis mediated by an aspartyl protease activity pharmacologically distinct from  $\gamma$ -secretase. *J. Neurochem.* 85, 1563–1574.
- (32) Sato, C., Morohashi, Y., Tomita, T., and Iwatsubo, T. (2006) Structure of the catalytic pore of  $\gamma$ -secretase probed by the accessibility of substituted cysteines. *J. Neurosci.* 26, 12081–12088.
- (33) Sato, C., Takagi, S., Tomita, T., and Iwatsubo, T. (2008) The C-terminal PAL motif and transmembrane domain 9 of presenilin 1 are involved in the formation of the catalytic pore of the  $\gamma$ -secretase. *J. Neurosci.* 28, 6264–6271.
- (34) Takagi, S., Tominaga, A., Sato, C., Tomita, T., and Iwatsubo, T. (2010) Participation of transmembrane domain 1 of presenilin 1 in the catalytic pore structure of the  $\gamma$ -secretase. *J. Neurosci.* 30, 15943–15950.
- (35) Tolia, A., Chavez-Gutierrez, L., and De Strooper, B. (2006) Contribution of presenilin transmembrane domains 6 and 7 to a water-containing cavity in the  $\gamma$ -secretase complex. *J. Biol. Chem.* 281, 27633–27642.
- (36) Chavez-Gutierrez, L., Tolia, A., Maes, E., Li, T., Wong, P. C., and de Strooper, B. (2008) Glu(332) in the Nicastrin ectodomain is essential for  $\gamma$ -secretase complex maturation but not for its activity. *J. Biol. Chem.* 283, 20096–20105.
- (37) Dries, D. R., Shah, S., Han, Y. H., Yu, C., Yu, S., Shearman, M. S., and Yu, G. (2009) Glu-333 of nicastrin directly participates in  $\gamma$ -secretase activity. *J. Biol. Chem.* 284, 29714–29724.
- (38) Futai, E., Yagishita, S., and Ishiura, S. (2009) Nicastrin is dispensable for  $\gamma$ -secretase protease activity in the presence of specific presenilin mutations. *J. Biol. Chem.* 284, 13013–13022.
- (39) Zhao, G., Liu, Z., Ilagan, M. X., and Kopan, R. (2010)  $\gamma$ -Secretase composed of PS1/Pen2/Aph1a can cleave notch and amyloid precursor protein in the absence of nicastrin. *J. Neurosci.* 30, 1648–1656.
- (40) Pardossi-Piquard, R., Yang, S. P., Kanemoto, S., Gu, Y., Chen, F., Bohm, C., Sevalle, J., Li, T., Wong, P. C., Checler, F., Schmitt-Ulms, G., St George-Hyslop, P., and Fraser, P. E. (2009) APH1 polar transmembrane residues regulate the assembly and activity of presenilin complexes. *J. Biol. Chem.* 284, 16298–16307.
- (41) Chen, A. C., Guo, L. Y., Ostaszewski, B. L., Selkoe, D. J., and LaVoie, M. J. (2010) Aph-1 associates directly with full-length and C-terminal fragments of  $\gamma$ -secretase substrates. *J. Biol. Chem.* 285, 11378–11391.
- (42) Hasegawa, H., Sanjo, N., Chen, F., Gu, Y. J., Shier, C., Petit, A., Kawarai, T., Katayama, T., Schmidt, S. D., Mathews, P. M., Schmitt-Ulms, G., Fraser, P. E., and St George-Hyslop, P. (2004) Both the sequence and length of the C terminus of PEN-2 are critical for intermolecular interactions and function of presenilin complexes. *J. Biol. Chem.* 279, 46455–46463.
- (43) Bergman, A., Hansson, E. M., Pursglove, S. E., Farmery, M. R., Lannfelt, L., Lendahl, U., Lundkvist, J., and Naslund, J. (2004) Pen-2 is sequestered in the endoplasmic reticulum and subjected to ubiquitylation and proteasome-mediated degradation in the absence of presenilin. *J. Biol. Chem.* 279, 16744–16753.
- (44) Cadwell, K., and Coscoy, L. (2005) Ubiquitination on nonlysine residues by a viral E3 ubiquitin ligase. *Science* 309, 127–130.
- (45) Burr, M. L., van den Boomen, D. J., Bye, H., Antrobus, R., Wiertz, E. J., and Lehner, P. J. (2013) MHC class I molecules are preferentially ubiquitinated on endoplasmic reticulum luminal residues during HRD1 ubiquitin E3 ligase-mediated dislocation. *Proc. Natl. Acad. Sci. U.S.A.* 110, 14290–14295.
- (46) Kim, S. H., and Sisodia, S. S. (2005) Evidence that the “NF” motif in transmembrane domain 4 of presenilin 1 is critical for binding with PEN-2. *J. Biol. Chem.* 280, 41953–41966.
- (47) Uemura, K., Lill, C. M., Li, X., Peters, J. A., Ivanov, A., Fan, Z., DeStrooper, B., Bacskai, B. J., Hyman, B. T., and Berezovska, O. (2009) Allosteric modulation of PS1/ $\gamma$ -secretase conformation correlates with amyloid  $\beta$ (42/40) ratio. *PLoS One* 4, e7893.
- (48) Fassler, M., Zocher, M., Klare, S., de la Fuente, A. G., Scheuermann, J., Capell, A., Haass, C., Valkova, C., Veerappan, A., Schneider, D., and Kaether, C. (2010) Masking of transmembrane-based retention signals controls ER export of  $\gamma$ -secretase. *Traffic* 11, 250–258.
- (49) Kim, J. H., Johannes, L., Goud, B., Antony, C., Lingwood, C. A., Daneman, R., and Grinstein, S. (1998) Noninvasive measurement of the pH of the endoplasmic reticulum at rest and during calcium release. *Proc. Natl. Acad. Sci. U.S.A.* 95, 2997–3002.

- (50) Baulac, S., LaVoie, M. J., Kimberly, W. T., Strahle, J., Wolfe, M. S., Selkoe, D. J., and Xia, W. (2003) Functional gamma-secretase complex assembly in Golgi/trans-Golgi network: Interactions among presenilin, nicastrin, Aph1, Pen-2, and  $\gamma$ -secretase substrates. *Neurobiol. Dis.* 14, 194–204.